THERMOCHEMICAL AND KINETIC ANALYSIS OF THE ALLYL RADICAL WITH O_2 REACTION SYSTEM

Jongwoo Lee and Joseph W. Bozzelli

Department of Environmental Science and Chemistry,
New Jersey Institute of Technology, Newark, NJ 07102

Introduction

Olefins (Alkenes) are major initial products from pyrolysis, oxidation or photochemical reactions of alkanes and ethers. The double bond in alkenes provides both an unsaturated site for addition reactions and an allylic site for facile abstractions, where the corresponding activation energy is lowered due to electron delocalization on the radical formed. The stability and low reactivity of these alkenyl radicals have been connected to the antiknock effect of fuel additives such as ethyl tert-butyl ether (ETBE).[1] The relatively high octane ratings for olefin blending suggest that olefins play an important role in pre-ignition chemistry related to engine knock. It is valuable to understand the fundamental chemical reaction pathways and kinetics of olefin oxidation in moderate to low temperature combustion chemistry for model development.

Ruiz et al.,[2] Morgan et al.,[3] and Slagle et al.[4,5] have reported the R—O_2 bond energy (17.2, 18.2, 18.4 kcal/mol, respectively) for the allyl (CH_2CHCH_2•, • : radical site) radical. Walker and co-workers[6,7] had studied at a total pressure of 60 Torr between 400 and 520 °C, where the equilibrium in the R + O_2 ⇔ RO_2 addition reaction is shifted to left, the rate constants of the CH_2CHCH_2• + O_2 → products reaction are significantly lower than those observed in the case of alkyl radicals. Baldwin et al.[8] and Lodhi and Walker[6] reported similarly low rate constants for the substituted allyl radicals, $CH_3CH_2CHCHCH_2$• and $CH_3CHCHCH_2$• reactions with O_2. Knyazev and Slagle[5] also studied the kinetics of the reaction $CH_3CHCHCH_2$• + O_2 ⇔ $CH_3CHCHCH_2O_2$• using laser photolysis/photoionization mass spectrometry. Room temperature decay constants of the $CH_3CHCHCH_2$• radical were determined in time-resolved experiments as a function of bath gas density ([He] = (3-24) × 10^{16} molecule cm^{-3}) and the rate constant at 297 K is k = (6.42 ± 0.54) × 10^{-13} cm^3/ (molecule s). At high temperatures (600 – 700K), no reaction of $CH_3CHCHCH_2$• with O_2 could be observed and upper limits to the rate constants were determined (1 × 10^{-16} cm^3/ (molecule s) at 600 K and 2 × 10^{-16} cm^3/ (molecule s) at 700 K).

Chen et al.[9] studied allylic isobutenyl radical with O_2. They reported the forward and reverse rate constants for initiation reaction, $CH_2C(CH_3)_2H$ + O_2 ⇔ $CH_2C(CH_3)_2$• + HO_2 to be 1.86 × 10^9 × $T^{1.301}$ × exp(-40939 cal/RT) cm^3/ (mol s) and 6.39 × 10^8 × $T^{0.944}$ × exp(-123.14 cal/RT) cm^3/ (mol s), respectively. They also proposed an important new reaction path, $CH_2C(CH_2$•$)COOH$ ⇔ $CH_2C(CH_2$•$)CO$• + OH ⇔ $CH_2Y(\underline{CCOC})$ + OH, for methylene oxirane formation.

This study focuses on the reaction mechanism of the allyl radical association with O_2. Thermochemical properties are estimated for reactants, intermediates, products and transition states in the reaction paths using *ab initio* and density functional calculations. The thermochemical parameters are used to calculate high-pressure limit rate constants using canonical Transition State Theory (TST). Rate constants as a function of temperature and pressure are estimated using a multifrequency quantum RRK analysis for k(E) and master equation for falloff. The data at relevant pressures and temperatures should be useful to both atmospheric and combustion models.

Calculation methods

Enthalpies of formation ($\Delta H_f°_{298}$) for reactants, intermediate radicals, transition states and products are calculated using the CBS-Q//B3LYP/6-31G(d,p) composite method and density functionals. The initial structure of each compound or transition state is determined using ROHF or UHF/PM3 in MOPAC,[10] followed by optimization and vibrational frequency calculation at B3LYP/6-31G(d,p) level of theory using GAUSSIAN 98.[11] Transition state geometries are identified by the existence of only one imaginary frequency, structure information and the TST reaction coordinate vibration information. Zero-point vibrational energies (ZPVE) are scaled by 0.9806 as recommended by Scott and Radom.[12] Single point energy calculations are carried out at the B3LYP/6-31G(d,p), /6-311+G(d,p), or /6-311++G(d,p). The CBS-Q method of Petersson and co-workers for computing accurate energies[13,14] is chosen as the determining enthalpies used in our kinetic analysis.

The CBS-Q//B3LYP/6-31G(d,p) calculation sequence is illustrated in Scheme 1 [Corrections for unpaired electron and spin contamination in intermediate overlap (i.e., $0< {}^{\alpha\beta}S_{ij} <1$) between the α- and β-spin orbitals[15] are included].

Scheme 1. CBS-Q//B3LYP/6-31G(d,p) Calculation Sequence

	Level of Theory
Optimized Geometry	B3LYP/6-31G(d,p)
Single Point Calculation	QCISD(T)/6-31+G(d')
	MP4(SDQ)/CBSB4
	MP2/CBSB3 CBSExtrap = (Nmin=10,Pop)

Determination of enthalpy of formation. The method of isodesmic reactions is used to determine the enthalpy of formation ($\Delta H_f°_{298}$) for parent and radical species. It provides higher accuracy for estimates of $\Delta H_f°_{298}$ than heats of atomization does.[16-18]

CH_2=CHCH$_2$OOH + CH_3CH_3 ⇔ CH_2=$CHCH_3$ + C_2H_5OOH (IR1)
CH_2=CHCH$_2$OO• + C_2H_5OH ⇔ CH_2=$CHCH_2OH$ + C_2H_5OO• (IR2)
C•H=CHCH$_2$OOH + C_2H_4 ⇔ CH_2=$CHCH_2OOH$ + C_2H_3• (IR3)
CH_2=C•CH$_2$OOH + CH_2=$CHCH_3$ ⇔ CH_2=$CHCH_2OOH$ + CH_2=C•CH_3 (IR4)
Y$\underline{CCCOO}$ + $(CH_3)_3CH$ ⇔ CY$\underline{CCOOC}$ + $CH_3CH_2CH_3$ (IR5)
Y$\underline{CC•COO}$ + CY$\underline{CCOOC}$ ⇔ Y$\underline{CCCOO}$ + CY$\underline{C•COOC}$ (IR6)
HOCH$_2$Y$\underline{CCO}$ + CH_3CH_3 ⇔ Y$\underline{CCO}$ + $(CH_3)_2C(OH)H$ (IR7)
O•CH$_2$Y$\underline{CCO}$ + CH_3OH ⇔ $HOCH_2Y\underline{CCO}$ + CH_3O• (IR8)

Ab initio calculations for ZPVE and thermal correction energy are performed on all of four compounds in the reaction. The three reference compounds in the working reaction (IR1), excepting the target molecule, CH_2=$CHCH_2OOH$ in (IR1), have experimental or theoretical determined values of $\Delta H_f°_{298}$. The unknown $\Delta H_f°_{298}$ of CH_2=$CHCH_2OOH$ is obtained with the calculated $\Delta H°_{rxn(298)}$ and known $\Delta H_f°_{298}$ of the three reference compounds. The other parent and radical species are calculated in the same manner.

Determination of entropy and heat capacity. The contributions of external rotations, translations, and vibrations to entropies and heat capacities are calculated from scaled vibration frequencies and moments of inertia for the optimized B3LYP/6-31G(d,p) structures. The number of optical isomers and spin degeneracy of unpaired electrons are also incorporated. Contributions from hindered internal rotation for S and $Cp(T)$ are determined using direct integration over energy levels of the intramolecular rotational potential curves. A program, "ROTATOR[19]", is used for calculation

of the energy levels. This technique employs expansion of the hindrance potential in the Fourier series (Eq. I), calculation of the Hamiltonian matrix on the basis of wave functions of the free internal rotor, and subsequent calculation of energy levels by direct diagonalization of the Hamiltonian matrix.[20,21] The torsional potential calculated at discrete torsion angles is represented by a truncated Fourier series:

$$V(\Phi) = a_0 + \Sigma\, a_i \cos(i\Phi) + \Sigma\, b_i \sin(i\Phi) \quad i = 1, 2, 3, \ldots \quad \text{(Eq. I)}$$

Values of the coefficients (a_0, a_i and b_i) are calculated to provide the minimum and maximum of the torsional potentials with allowance of a shift of the theoretical extreme angular positions.[20,21]

High-pressure limit A factor (A) and rate constant (k_∞) determination. For the reactions where thermochemical properties of transition state are calculated by ab initio or density functional methods, k_∞'s are fit by three parameters A, n, and *Ea* over temperature range from 298 to 2000K, $k_\infty = A\,(T)^n \exp(-Ea/RT)$. Entropy differences between reactant and transition state are used to determine the pre-exponential factor, A, via canonical Transition State Theory (TST)

$$A = (k_b T/h_p)\exp(\Delta S^{\ddagger}/R),\ Ea = \Delta H^{\ddagger}$$

(h_p is the Planck constant and k_b is the Boltzmann constant.) Treatment of the internal rotors for *S* and *Cp*(*T*) is important here because these internal rotors are often lost in the cyclic transition state structures.

Kinetic analysis. Thermochemical properties for each species on the potential energy surface for the reaction system are evaluated. Forward or reverse rate constants (high-pressure limit) for each, elementary reaction step are determined from the calculations and use of literature data for enthalpies of stable molecules. Reverse rate constants are calculated from microscopic reversibility.

Multifrequency quantum Rice-Ramsperger-Kassel (QRRK) analysis is used to calculate *k*(E) with a master equation analysis[22] for fall-off in order to obtain rate constants as a function of temperature and pressure. This kinetic analysis is for the chemical activation and the dissociation reaction systems. The master equation analysis[22] uses an exponential-down model for the energy transfer function with $(\Delta E)^\circ_{down}$ = 1000 cal/mol,[23,24] for N_2 as the third body and a 500 cal energy grain is used.

The QRRK/master equation analysis is described by Chang et al.[22,25] Further validated by recent work of Sun et al. ((JP030667l) in press 2003). The QRRK code utilizes a reduced set of three vibration frequencies which accurately reproduce the molecules' heat capacity; the code includes contribution from one external rotation in calculation of the ratio of the density of states to the partition coefficient ρ(E)/Q. Comparisons of ratios of these ρ(E)/Q with direct count ρ(E)/Q's have been shown to result in good agreement.[26] Rate constant results from the quantum RRK-Master equation analysis are shown to accurately reproduce (model) experimental data on several complex systems. They also provide a reasonable method to estimate rate constants for numerical integration codes by which the effects of temperature and pressure can be evaluated in complex reaction systems.

Results and Discussion

Enthalpy of formation ($\Delta H_f°_{298}$). The enthalpies of formation for $CH_2{=}CHCH_2OOH$ are –13.53 and –13.49 kcal/mol by B3LYP/6-31G(d,p) and CBSQ//B3LYP/6-31G(d,p), respectively. The enthalpy of formation for the parent hydroperoxide is important because it allows the evaluation of peroxy radicals.

The bond energies of $CH_2{=}CHCH_2OOH$, $C(OOH)H_2CHO$,[27] C_2H_5OOH,[22] and $CH_3C(=O)OOH$[28] are compared in **Table 1**. The R–OOH bond energy in $CH_2{=}CHCH_2OOH$ is 14 kcal/mol lower than that of C_2H_5OOH, because the radical site is resonantly stabilized. The RO–OH and ROO–H bonds in $CH_2{=}CHCH_2OOH$ are 45.4 and 86.6 kcal/mol, similar to those in C_2H_5OOH, 45.1 and 85.3 kcal/mol, respectively.

Table 1. Comparison of Bond Energies between Allyl Hydroperoxide and three C2 Hydroperoxide

(Units in kcal/mol)	**$CH_2{=}CHCH_2OOH$**	$C(OOH)H_2CHO$	C_2H_5OOH	$CH_3C(=O)OOH$
ROO—H	**86.61**	87.28	85.27	98.33
RO—OH	**45.39**	45.13	45.12	50.95
R—OOH	**57.05**	63.21	71.35	85.22
H--CH=$CHCH_2OOH$	**112.36**	n/a	n/a	n/a
CH_2=C(--H)CH_2OOH	**110.17**	n/a	n/a	n/a
$C(OOH)H_2C(=O)$--H,	n/a	88.65	n/a	n/a
H--CH_2CH_2OOH,	n/a	n/a	103.21	n/a
H--$CH_2C(=O)OOH$	n/a	n/a	n/a	103.95

Entropy ($S^o_{(298)}$) and heat capacity ($Cp(T)$, 300 ≤ T/K ≤ 1500). Entropy and heat capacities are calculated based on vibration frequencies and moments of inertia of the optimized B3LYP/6-31G(d,p) structures. Symmetry, number of optical isomers and electronic spin are incorporated in estimation of $S^o_{(298)}$. Torsion frequencies are omitted in these calculations, instead, contributions from internal rotation for $S^o_{(298)}$ and *Cp*(*T*)'s are determined, using direct integration over energy levels of the intramolecular rotational potential curves[20,21].

Potential energy diagram for $CH_2{=}CHCH_2\bullet + O_2$ reaction system. The energy diagram for the allyl ($CH_2{=}CHCH_2\bullet$) + O_2 reaction is illustrated in two **Figures 1 and 2**. The reactions involving intramolecular hydrogen transfer and direct HO_2 elimination are illustrated in **Figure 1**. Reactions involving peroxy radical addition to each of the π bond carbons, ring formation, and subsequent reactions of the two cyclic peroxide alkyl radicals are illustrated in **Figure 2**. The 14 reaction paths, 6 reaction intermediates, and 14 transition states are illustrated. Enthalpies of formation are from CBSQ// B3LYP/6-31G(d,p) calculations and in units of kcal/mol. Transition state enthalpies are relative to the corresponding stabilized adduct.

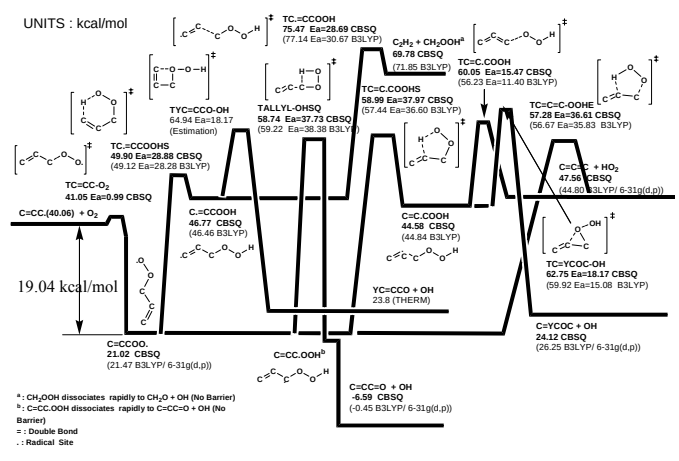

Figure 1. Potential energy I of II for allyl + O_2 (I) Isomerizations via H shifts.

The allyl radical adds to O_2 (*Ea* = 0.99) to form an energized peroxy adduct [$CH_2{=}CHCH_2OO\bullet$]* with a shallow well (ca. 19

kcal/mol); which predominantly dissociates back to reactants under combustion conditions. The reaction channels of the $[CH_2{=}CHCH_2OO\bullet]^*$ adduct include reverse reaction to reactants, stabilization to $CH_2{=}CHCH_2OO\bullet$ radical ($\Delta H_f°_{298}$ = 21.02), decomposition to products, $CH_2{=}C{=}CH_2 + HO_2$ via direct HO_2 elimination with a barrier (*Ea* = 36.61), isomerizations via hydrogen shifts to form $C\bullet H{=}CHCH_2OOH$ or $CH_2{=}C\bullet CH_2OOH$ isomers ($\Delta H_f°_{298}$ = 46.77 or 44.58, respectively) with barriers (*Ea* = 28.88 or 37.97, respectively), or a hydrogen transfer (*Ea* = 37.73) from the ipso carbon to the peroxy radical to form the unstable intermediate $\{CH_2{=}CHC\bullet HOOH\}$, which immediately dissociates to more stable products, 2-propenal plus OH.

The $C\bullet H{=}CHCH_2OOH$ isomer can undergo β scission to products, ($C_2H_2 + \{C\bullet H_2OOH\} \rightarrow C_2H_2 + CH_2O + OH$) (*Ea* = 37.73), a ring closure to form the unstable intermediate {Y<u>CCCO</u>} plus OH, (Y = <u>cyclic</u>) which rapidly dissociates to more stable products, 2-propenal plus OH, or isomerize via a hydrogen shift (*Ea* = 3.13) to form a $CH_2{=}CHCH_2OO\bullet$ isomer.

The $CH_2{=}C\bullet CH_2OOH$ isomer can undergo β scission to products, $CH_2{=}C{=}CH_2 + HO_2$ (*Ea* = 15.47), a ring closure to form methyene oxirane plus OH radical (*Ea* = 18.17), or isomerize via a hydrogen shift (*Ea* = 14.41) to form a $CH_2{=}CHCH_2OO\bullet$ isomer.

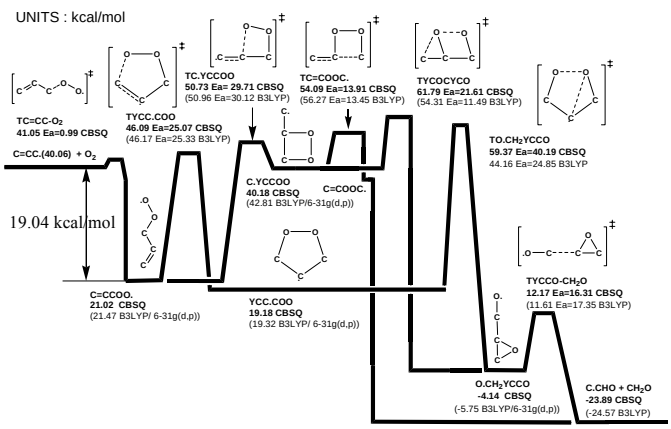

Figure 2. Potential energy II of II for allyl + O_2 (II) Cyclization pathways to form cyclic adducts and further reactions.

Intramolecular peroxy radical addition to sp^2 hybridized carbons - cyclization reaction paths. The $[CH_2{=}CHCH_2OO\bullet]^*$ adduct can also cyclize to four- or five-member cyclic peroxide-alkyl radicals, $C\bullet H_2Y$<u>CCOO</u> and <u>YCC•COO</u> ($\Delta H_f°_{298}$ = 40.18 and 19.18, respectively). $CH_2{=}CHCH_2OO\bullet$ cyclization to four- or five-member cyclic peroxides require barriers, *Ea* = 29.71 and 25.07, respectively), which have slightly higher barriers than reverse reaction (*Ea* = 20.03).

The $C\bullet H_2Y$<u>CCOO</u> adduct can undergo β scission to products, $C\bullet H_2CHO + CH_2O$ (*Ea* = 13.91), form a cyclic epoxide-alkoxy radical, $O\bullet CH_2Y$<u>CCO</u> ($\Delta H_f°_{298}$ = -4.14) via TY<u>COC</u>Y<u>CO</u> (*Ea* = 21.61), or undergo ring open to form $CH_2{=}CHCH_2OO\bullet$ adduct (*Ea* = 10.55). The $O\bullet CH_2Y$<u>CCO</u> intermediate will undergo β scission to products, $C\bullet H_2CHO + CH_2O$ via TY<u>CCO</u>-CH_2O (*Ea* = 16.31).

The 5-member ring Y<u>CC•COO</u> can also form the epoxide-alkoxy radical (above), $O\bullet CH_2Y$<u>CCO</u> via $TO\bullet CH_2Y$<u>CCO</u> (*Ea* = 40.19), undergo ring open to form $CH_2{=}CHCH_2OO\bullet$ adduct (*Ea* = 26.91). This cyclic Y<u>CC•COO</u> adduct further reacts with O_2 to chain branching products: $CH_2O + C(=O)HC(=O)H + OH$.

Comparison of $CH_2{=}CHC\bullet H_2$, $C\bullet H_2CHO$, C_2H_5, and $CH_3C\bullet O$ with O_2. The $CH_2{=}CHC\bullet H_2 + O_2$, $C\bullet H_2CHO + O_2$,[27] $C_2H_5 + O_2$,[22] and $CH_3C\bullet O + O_2$[28] reaction systems have significant differences. The $CH_2{=}CHC\bullet H_2 + O_2$ reaction system of this study has a lower well depth of 19.04 kcal/mol compared to $C\bullet H_2CHO + O_2$, $C_2H_5 + O_2$ and $CH_3C\bullet O + O_2$, which have well depths of 27.5, 35.3 and 35.5 kcal/mol, respectively.

The H shift barriers in the $CH_2{=}CHCH_2OO\bullet$, $C(OO\bullet)H_2CHO$ and $CH_3C(=O)OO\bullet$ peroxy radicals are lower than those of concerted HO_2 elimination, whereas in $C_2H_5OO\bullet$, direct HO_2 elimination has a lower barrier than the H shift.

The well depth and barriers of H shift and HO_2 elimination in the $CH_2{=}CHC\bullet H_2$, $C\bullet H_2CHO$, $C_2H_5\bullet$, and $CH_3C\bullet O$ with O_2 reaction systems are compared in **Table 2**.

Table 2. Comparison of $CH_2{=}CHC.H_2$, $C.H_2CHO$, C_2H_5, and $CH_3C.(=O)$ with O_2

(Units in kcal/mol)		$CH_2{=}CHC.H_2 + O_2$	$C.H_2CHO + O_2$	$C_2H_5 + O_2$	$CH_3C.(=O) + O_2$
Well Depth		**19.04**	27.5	35.3	35.5
Barrier in	1) H Shift[a]	**28.88**	20.25	36.36	26.42
	2) HO_2 Elimination[a]	**36.61**	48.31	30.48	34.58

[a] H shift and HO_2 elimination for the $CH_2{=}CHCH_2OO.$, $C(OO.)H_2CHO$, $C_2H_5OO.$, and $CH_3C(=O)OO.$

Kinetic analysis for allyl + O_2. The QRRK calculations for *k*(E) and master equation analysis for fall-off are performed on this allyl ($CH_2{=}CHCH_2\bullet$) + O_2 reaction system to estimate rate constants and to determine important reaction paths as a function of temperature and pressure. Rate constants at 1 atm pressure versus 1000/T are illustrated in **Figure 3**. Stabilization $CH_2{=}CHCH_2OO\bullet$ is important below 600 K, with reverse dissociation above 600 K. $CH_2{=}CHCH_2OO\bullet$ adduct, cyclic isomers, and H-shift isomers exhibit significant falloff at higher temperatures (above 800 K). Allene + HO_2 products via a HO_2 molecular elimination path, Y<u>CC•COO</u> via cyclization, and H transfer from primary vinyl group to peroxy radical; then β-scission reaction leading to $C_2H_2 + CH_2O + OH$ are major product channels at higher temperatures (above 600 K).

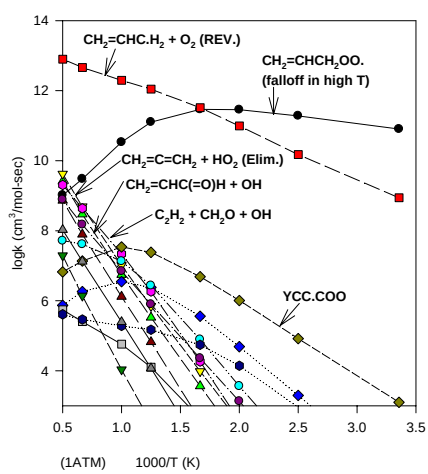

Figure 3. $CH_2{=}CHCH_2 + O_2$ -> products *k* vs. 1000/T at 1 atm.

Conclusions

Thermochemical properties for important species in the allyl radical (CH_2=$CHCH_2$•) + O_2 reaction system are calculated using density functional and *ab initio* methods. Enthalpies of formation ($\Delta H_f°_{298}$) are determined using isodesmic reactions at the CBSQ level. Entropies ($S°_{298}$) and heat capacities ($Cp(T)$) include internal rotor contributions.

The CH_2=CHC•H_2 + O_2 reaction system is found to have a relatively shallow well depth of 19.04 kcal/mol and all product formation pathways from the peroxy radical, involve barriers that are above the energy of the initial reactants. Major reaction paths at 1 atm pressure are stabilization of the peroxy adduct (CH_2=$CHCH_2$OO•) below 600 K, with reverse dissociation above 600 K. Important reaction products are allene + HO_2 products via a HO_2 molecular elimination, Y<u>CC•COO</u> which dissociates or further reacts to chain branching products. C•H=$CHCH_2$OOH from hydrogen transfer, which undergoes β-scission reaction leading to C_2H_2 + CH_2O + OH is important product channel above 600 K.

Acknowledgements. We acknowledge the USEPA Northeast Regional Research Center and the USEPA Airborne Organics Research Center for funding. We would also like to thank to C. Sheng for the SMCPS program.

References

(1) Bach, R. D.; Ayala, P. Y.; Schlegel, H. B. *J. Am. Chem. Soc.* **1996**, *118*, 12758.
(2) Ruiz, R. P.; Bayes, K. D.; Macpherson, M. T.; Pilling, M. J. *J. Phys. Chem.* **1981**, *85*, 1622.
(3) Morgan, C. A.; Pilling, M. J.; Tulloch, J. M.; Ruiz, R. P.; Bayes, K. D. *J. Chem. Soc. Faraday Trans. 2* **1982**, *78*, 1323.
(4) Slagle, I. R.; Ratajczak, E.; Heaven, M. C.; Gutman, D.; Wagner, A. F. *J. Am. Chem. Soc.* **1985**, *107*, 1838.
(5) Knyazev, V. D.; Slagle, I. R. *J. Phys. Chem. A* **1998**, *102*, 8932.
(6) Lodhi, Z. H.; Walker, R.W. *J. Chem. Soc., Faraday Trans.* **1991**, *87*, 681.
(7) Stothard, N. D.; Walker, R. W. *J. Chem. Soc. Faraday Trans.* **1992**, *88*, 2621.
(8) Baldwin, R. R.; Bennett, J. P.; Walker, R. W. *J. Chem. Soc. Faraday Trans. 1* **1980**, *76*, 2396.
(9) Chen, C.; Bozzelli, J. W. *J. Phys. Chem. A* **2000**, *104*, 9715.
(10) Stewart, J .J. P. MOPAC 6.0, J. Frank Seiler Research Lab., US Air Force Academy: Colorado, **1990**.
(11) Frisch, M. J.; Trucks, G. W.; Schlegel, H. B.; Scuseria, G.; Robb,M. A.; Cheesman, J. R.; Zakrzewski, V. G.; Montgomery, J. A., Jr.; Stratmann, R. E.; Burant, J. C.; Dapprich, S.; Millam, J. M.; Danicls, A. D.; Kudin, K. N.; Strain, M. C.; Farkas, O.; Tomasi, J.; Baronc, V.; Cossi, M.; Cammi, R.; Mennucci, B.; Pomelli, C.; Adamo, C.; Clifford, S.; Ochterski, J.; Petersson, G. A.; Ayala, P. Y.; Cui, Q.; Morokuma, K.; Malick, D. K.; Rabuck, A. D.; Raghavachari, K.; Froesman, J. B.; Cioslowski, J.; Ortiz, J. V.; Baboul, A. G.; Stefanov, R. B.; Liu, G.; Liashenko, A.; Piskorz, P.; Komaromi, I.; Gomperts, R.; Matrin, R. L.; Fox, D. J.; Keith, T.; Al-Laham, M. A.; Peng, C. Y.; Nanayakkara, A.; Gonzalez, C.; Challacombe, M.; Gill, P. M. W.; Johnson, B.; Chen, W.; Wong, M. W.; Andres, J. L.; Head-Gordon, M.; Pople, J. A. *Gaussian 98*; Gaussian Inc.: Pittsburgh, PA, **1998**.
(12) Scott, A. P.; Radom, L. *J. Phys. Chem.* **1996**, *100*, 16502.
(13) Nyden, M. R.; Petersson, G. A. *J. Chem. Phys.* **1991**, *75*, 1843.
(14) Petersson, G. A. *J. Chem. Phys.* **1994**, *94*, 6081.
(15) Montgomery Jr., J. A.; Petersson, G. A. *J. Phys. Chem.* **1994**, 101, 5900.
(16) Hehre, W. J.; Radom, L.; Schleyer, P. R.; Pople, J. A. *Ab-Initio Molecular Orbital Theory*, John Wiley & Sons: New York, NY, 1986.
(17) Lay, T. H.; Bozzelli, J. W. *J. Phys. Chem. A* **1997**, *101*, 9505.
(18) Sun, H.; Bozzelli, J. W. *J. Phys. Chem. A* **2001**, *105*, 4504.
(19) Shokhirev, N. V. http://www.chem.arizona.edu/faculty/walk/nikolai/programs.html #programs July, 2002.
(20) Lay, T. H.; Krasnoperov, L. N.; Venanzi, C. A.; Bozzelli, J. W. *J. Phys. Chem.* **1996**, *100*, 8240.
(21) Yamada, T.; Lay, T. H.; Bozzelli, J. W. *J. Phys. Chem. A* **1999**, *103*, 5602.
(22) Sheng, C. Y.; Bozzelli, J. W.; Dean, A. M.; Chang, A. Y. *J. Phys. Chem. A* **2002**, *106*, 7276.
(23) Troe, J. *In Combustion Chemistry*, W.C. Gardiner Jr., Ed.; Springer-Verlag: New York, 1984.
(24) Knyazev, V. D.; Slagle, I. R. *J. Phys. Chem.* **1996**, *100*, 5318.
(25) Chang, A. Y.; Bozzelli, J. W.; Dean, A. M. *Int. J. Res. Phys. Chem. Chem. Phys. (Zeit. Phys. Chem)* **2000**, *214*, 1533.
(26) Bozzelli, J. W.; Chang, A. Y.; Dean, A. M. *Int. J. Chem. Kinet.* **1997**, *29*, 161.
(27) Lee, J.; Bozzelli, J. W. *J. Phys. Chem. A* **2003**, *107*, 3778.
(28) Lee, J.; Chen, C.; Bozzelli, J. W. *J. Phys. Chem. A* **2002**, *106*, 7155.